DOE/PC/90185--T4

DE92 012645

# QUARTERLY PROGRESS REPORT

October 1, 1991 - December 31, 1991

Principal Investigator: Mark W. Richman

Contract Number: DE-AC22-91PC90185

# Introduction

In this quarter we accomplished two milestones. First, we qualitatively compared the approximate solutions for gravity-driven granular flows down bumpy inclines obtained by Richman and Marciniec [1990] to the experimental results for the same flows obtained Johnson and Jackson [1990]. The comparison was made by employing the reparameterized solutions of Richman and Marciniec [1990] and by analyzing several angles of inclination, coefficients of restitution, and boundary geometries. The results of the comparison are summarized in the attached paper (Granular Flows Down Bumpy Inclines, by Richman, M.W. and Martin, R.E.) presented at the Joint DOE-NSF Workshop on the Flows of Particulates and Fluids held at Worcester Polytechnic Institute on October 22-24, 1991.

Next, we obtained exact numerical solutions the equations of motion that were solved approximately by Richman and Marciniec [1990]. Exact solutions to the governing equations require that the stresses and energy flux vanish at the top of the flow, and satisfy separate momentum and energy balances at the base of the flow. In order to generate numerical solutions, we relaxed very slightly the normal stress condition at the top, assigned a value to the granular temperature there, and, for those inclinations, flow particles, and boundaries that admitted solutions, calculated the profiles of solid fraction, granular temperature, and velocity and the corresponding values of mass

flow rate and mass hold-up. In this manner we found that there are flow rates at which two flows are possible. Of the two, the less massive is more dilute, more thermalized, and faster than its more massive counterpart. In addition we found that the approximate results obtained by Richman and Marciniec [1990] for the same flows are in reasonable agreement with the numerical solutions.

In what follows, we outline this numerical work in detail.

## The Boundary Value Problem

Of interest here are steady, fully developed, gravity-driven flows of identical, smooth spheres down bumpy inclined surfaces. The diameter of each sphere is $\sigma$, the mass density of each is $\alpha$, and the coefficient of restitution between them is e. The vertical acceleration due to gravity is g, the angle between the incline and the horizontal is $\phi$, and the perpendicular distance from the incline to the free surface is L. We introduce an $x_1$-$x_2$-$x_3$ Cartesian coordinate system in which $x_1$ measures parallel distances along the incline, and $x_2$ measures perpendicular distances above the incline. In these flows, the solid fraction $\nu$, the dimensionless counterpart $u=u_1/(\sigma g)^{1/2}$ to the $x_1$-velocity component $u_1$, and the dimensionless measure $w=(T/\sigma g)^{1/2}$ of the granular temperature T depend only on the dimensionless coordinate $y=(L-x_2)/\sigma$. The y-coordinate varies from 0 at the free surface to the dimensionless depth $\beta \equiv L/\sigma$ at the base of the

incline.

In these flows, the balance of mass and the $x_3$-component of the balance of momentum are identically satisfied. Furthermore, if $P_{12}$ and $P_{22}$ are the $x_1$-$x_2$ and $x_2$-$x_2$ components of the pressure tensor, then in terms of their dimensionless counterparts $S \equiv -P_{12}/\alpha\sigma g$ and $N \equiv P_{22}/\alpha\sigma g$ the $x_1$-component of the momentum equation is

$$S' = \nu \sin\phi \quad , \tag{1}$$

where a prime denotes differentiation with respect to y, and the $x_2$-component of the momentum equation is

$$N' = \nu \cos\phi \quad . \tag{2}$$

Regardless of $\nu(y)$, y may be eliminated between equations (1) and (2) to show that $S/N = \tan\phi$ provided that S and N vanish at the free surface. Finally, if $Q_2$ is the $x_2$-component of the energy flux, and $\gamma$ is the collisional rate of energy dissipation, then in terms of their dimensionless counterparts $q \equiv Q_2/\alpha(\sigma g)^{3/2}$ and $\Gamma \equiv \gamma/\alpha\sigma^{1/2}g^{3/2}$ the energy equation is

$$q' - Su' - \Gamma = 0 \quad . \tag{3}$$

Constitutive relations for S, N, q, and $\Gamma$ are necessary to close equations (1), (2), and (3).

Here we employ the constitutive theory of Jenkins and Richman [1985], which is restricted to smooth, nearly elastic

spheres but includes the effects of particle transport and particle collisions. According to this theory, the normal pressure is given by

$$N = 4\nu GFw^2 \quad , \tag{4}$$

where $G \equiv \nu(2-\nu)/2(1-\nu)^3$ and $F \equiv 1+1/4G$, and the gradient of velocity is given in terms of the stress ratio by

$$u' = \frac{-5\pi^{1/2}FSw}{2EN} \quad , \tag{5}$$

where $E \equiv 1+\pi(1+5/8G)^2/12$. The corresponding constitutive relations for q and $\Gamma$ are

$$q = \frac{2MNw'}{\pi^{1/2}F} \quad , \tag{6}$$

in which $M \equiv 1+9\pi(1+5/12G)^2/32$, and

$$\Gamma = \frac{6(1-e)Nw}{\pi^{1/2}F} \quad . \tag{7}$$

Following Richman and Marciniec [1990], we employ equations (5), (6), and (7) to eliminate u', q, and $\Gamma$ from equation (3), and differentiate equation (4) to write $\nu'$ in terms of N'and w'. In this manner, we find that in terms of the measure h of energy flux defined by

$$w' = hw \quad , \tag{8}$$

the energy equation becomes

$$h' = \lambda^2 - \frac{(1-2H)N'}{N}h - (1+4H)h^2 \quad , \tag{9}$$

where $\lambda^2$ is defined by the difference

$$\lambda^2 = \frac{1}{2M}\left[6(1-e) - \frac{5\pi F^2 S^2}{2EN^2}\right] \quad , \tag{10}$$

and H is the function of $\nu$ defined by

$$2H = \frac{-[d\ell n(M/F)/d\nu]}{[d\ell n(\nu GF)/d\nu]} \quad . \tag{11}$$

The quantity $\lambda^2$ is a local measure of the difference between the rate at which energy is dissipated by inelastic collisions and the rate at which energy is supplied to the flow by gravity. The function 2H, which decreases monotonically from 1 to 0 as $\nu$ increases from 0 to 1, measures the importance of the transport contributions to the fluxes of momentum and energy.

The boundary conditions at y=0 reflect the facts that the stresses and energy flux vanish there. That is,

$$S(0) = 0 \quad \text{and} \quad N(0) = 0 \quad , \tag{12}$$

and

$$h(0) = 0 \quad . \tag{13}$$

The boundary conditions at the $y=\beta$ depend on the bumpiness of the base. The incline of interest here is a flat surface to which smooth hemispherical particles of diameter d are randomly attached at an average distance s apart. The dimensionless parameters that determine the bumpiness of the boundary are the ratios $r\equiv\sigma/d$ and $\Delta\equiv s/d$. For given values of r, the full range of $\Delta$ is from -1, which corresponds to a perfectly flat boundary, to $-1+\sqrt{(1+2r)}$, which is the maximum value that prevents any flow particle from colliding with the flat part of the base. In a collision between a flow particle and a boundary particle, the distance between their centers is $\bar{\sigma}\equiv(\sigma+d)/2$ and the coefficient of restitution is $e_w$.

Conditions that express the balance of momentum and energy at these bumpy boundaries have been obtained by Richman [1988]. When applied to the flows of interest here, the balance of tangential momentum at the base determines the slip velocity $u(\beta)$ according to

$$\frac{u(\beta)}{w(\beta)} = \sqrt{\frac{\pi}{2}}\,\frac{S}{N}\,f \quad , \tag{14}$$

where the dependence of f on the boundary geometry and solid fraction at the boundary is given by

$$f = \frac{1-(5\bar{\sigma}F/2^{3/2}\sigma E)\,(1+\sigma B/\bar{\sigma})\sin^2\theta}{(2/3)\,[2\csc^2\theta(1-\cos\theta)-\cos\theta]} + \frac{5\bar{\sigma}F}{\sqrt{2}\sigma E} \quad , \tag{15}$$

in which $B \equiv \pi(1+5/8G)/12\sqrt{2}$ and $\sin\theta \equiv (1+\Delta)/(1+r)$. Similarly, the balance of energy at the base determines the gradient of the granular temperature according to

$$h(\beta) = b \quad , \tag{16}$$

where the dependence of b on the boundary geometry and solid fraction at the boundary is given by

$$b = \frac{F}{\sqrt{2}M}\left[\frac{\pi S^2}{2N^2}f - 2(1-e_w)(1-\cos\theta)\csc^2\theta\right] \quad . \tag{17}$$

The quantity b is the dimensionless difference between the slip work done by the boundary, and the collisional dissipation at the boundary. The boundary supplies fluctuation energy to the flow when b is positive and absorbs fluctuation energy when b is negative.

## Solution Procedure

Because the velocity has been eliminated from the energy equation and the stress ratio S/N is equal to $\tan\phi$, equations (2), (4), (8), and (9) are uncoupled from equations (1) and (5). Consequently, for fixed values of e, $e_w$, r, $\Delta$, and $\phi$, equations (2), (4), (8), and (9) determine the functions N(y), h(y), w(y), and $\nu$(y) to within three constants of integration. These three constants and the dimensionless depth $\beta$ are determined by the second of the stress conditions (12), energy flux conditions (13)

and (16), and by prescribing a nonzero value W of w at y=0. With $\nu(y)$ known, the mass hold-up corresponding to this choice of W may be calculated according to its definition,

$$m_t = \int_0^\beta \nu dy \quad , \tag{18}$$

and equation (1) may be integrated to determine S(y) to within a constant of integration that is fixed by the first of stress conditions (12). Alternatively, with N(y) known, S(y) is given simply by the product $N(y)\tan\phi$. Independent of the variation S(y) but with $\nu(y)$ and w(y) known, equation (5) may be integrated to determine u(y) to within a constant that is fixed by momentum flux condition (14). The corresponding mass flow rate m for the choice of W may then be calculated according to its definition,

$$\dot{m} = \int_0^\beta \nu u dy \quad . \tag{19}$$

We employ a fourth order Runge-Kutta technique to integrate equations (2), (4), (8), and (9) from y=0, where N and h vanish and w is equal to its free surface value W. In equation (9), we employ equations (2) and (4) to write the ratio N'/N as $\cos\phi/(1+4G)w^2$. Whenever necessary, we invert equation (4) to calculate the value of $\nu$ corresponding to known values of N and w. For any value of W, the depths $\beta$ are determined as those values of y at which the basal energy flux condition (16) is

satisfied. If this conditon is not satisfied within 1000 particle diameters from y=0, then we conclude that either no steady, fully developed solution exists for the value of W chosen, or that the depth of flow is nearly unbounded. If this condition is satisfied, then N(y), h(y), w(y), and $\nu$(y) are completely determined, and equations (1) and (5) may be integrated numerically to determine S(y) and u(y).

According to constitutive relation (4), $\nu$ must be equal to zero if N vanishes where w does not. In particular, $\nu$ must be equal to zero at y=0. Because h is also equal to zero there, equations (2), (8), and (9) demonstrate that N'(0), w'(0), and h'(0) each vanish at y=0. Integrations initiated from y=0 therefore yield no spatial variations in N, h, w, and $\nu$. This indicates that the flows are infinitely deep and that N, h, w, and $\nu$ each approach their values at y=0 asymptotically from the base. To overcome this difficulty, we set $\nu(0)$ equal to $10^{-6}$, which is equivalent to relaxing very slightly the normal stress condition at y=0, and allows the integrations to proceed away from zero. We have also initiated the integrations with several other values of $\nu(0)$ between $10^{-5}$ and $10^{-7}$, and in each case obtained results that were indistinguishable from those based on $\nu(0)=10^{-6}$.

## Results and Discussion

In Figure 1 we show the variations of $\dot{m}$ with W between 0 and

3 for $e=.8$, $e_w=.95$, $r=1/2$, and $\Delta=-1+\sqrt{2}$ at inclinations $\phi$ of 19.00°, 20.04°, 20.70°, 21.00°, and 21.50°. Steady, fully developed flows also occur at these inclinations when W is greater than 3. However, the solid fraction in these flows is everywhere less than .02. The theory predicts that when W is extremely small (<.02), the flows are unrealistically dense. In fact, the lowest value of W on each curve shown in Figure 1 corresponds to the minimum value at which the solid fraction everywhere within the flow is less than .65. As W increases from its minimum value, although the flow rates do not vary monotonically, the flows become monotonically more dilute.

In Figure 2 we show the variations of $\dot{m}$ with W for $e=.95$, $e_w=.8$, $r=1/2$, and $\Delta=-1+\sqrt{2}$ at inclinations of 11.56°, 11.80°, 12.00°, 12.20°, and 12.90°. Corresponding to each inclination is a finite maximum value of W at which $\dot{m}$ becomes unbounded. When $\phi=12.90°$, as W increases from its minimum value at which the solid fraction everywhere within the flow is less than .65 to its maximum value, the flows become increasingly more dilute. At the remaining inclinations, two flows at different flow rates are physically possible for fixed values of W near its minimum. As W increases from its minimum value, the flow at the higher flow rate becomes more dense until, at a value of W that is less than its maximum, the solid fraction somewhere in the flow reaches .65. The flow at the lower flow rate becomes more dilute as W increases to its maximum value.

To each value of W for which a steady, fully developed flow occurs, there corresponds a mass hold-up $m_t$ that may be calculated according to its definition (18). In Figure 3, for example, we eliminate W and show as a solid curve the variation of $\dot{m}$ with $m_t$ when $\phi=20.70°$ for the values $e=.8$, $e_w=.95$, $r=1/2$, and $\Delta=-1+\sqrt{2}$ taken from Figure 1. In Figure 4, we show as a solid curve the variation of $\dot{m}$ with $m_t$ when $\phi=12.20$ for the values $e=.95$, $e_w=.8$, $r=1/2$, and $\Delta=-1+\sqrt{2}$ taken from Figure 2. Also shown in Figures 3 and 4 as dashed curves are the corresponding approximate variations predicted by Richman and Marciniec [1990], who integrated the balance of momentum and energy by replacing the solid fraction by its depth averaged value wherever it occurred in equations (1), (2), and (9). For those flow rates at which steady, fully developed flows are predicted by both the numerical solution obtained here and the approximate solution obtained by Richman and Marciniec [1990], the values of $m_t$ predicted by the two agree quite well. However, according to Figure 3, there can be a considerable discrepancy between the two predictions concerning the range of flow rates within which steady flows are possible.

For the case $\phi=20.70°$ shown in Figures 1 and 3, there are two flows possible for fixed flow rates between the maximum 134.0 and 17.8; the less massive flow is more dilute, faster, and more thermalized than its more massive counterpart. As $\dot{m}$ decreases in this range, the flow at the higher mass hold-up becomes more

dense, slower, and less thermalized, until at $\dot{m}$=17.8 the solid fraction within the flow exceeds .65 and we assume that it can no longer be sheared. As $\dot{m}$ decreases from its maximum value to 1, the flow at the lower mass hold-up becomes more dilute, slower, and more thermalized. Qualitatively similar observations may be made for the other inclinations shown in Figure 1.

For the case $\phi$=12.20° shown in Figures 2 and 4, there are two steady, fully developed flows for fixed flow rates between the minimum 11.3 and 56.7. Of the two, the less massive is more dilute, faster, and more thermalized than its more massive counterpart. As $\dot{m}$ increases from 11.3 the less massive flow becomes more dilute, faster, and more thermalized. The more massive flow becomes more dense, faster, and only slightly less thermalized, until at $\dot{m}$=56.7 the solid fraction somewhere within the flow exceeds .65. Qualitatively similar observations may be made for the other inclinations shown in Figure 2.

In Figures 5, 6, and 7 we plot as solid curves the variations of $\nu$, w, and u with dimensionless distance Y≡y-$\beta$ from the base for the case $\phi$=20.70°, e=.8, $e_w$=.95, r=1/2, and $\Delta$=-1+$\sqrt{2}$ when $\dot{m}$=50. In Figures 8, 9, and 10 we do the same for the case $\phi$=12.20°, e=.95, $e_w$=.8, r=1/2 and $\Delta$=-1+$\sqrt{2}$. Shown as dashed curves in these figures are the corresponding approximate variations obtained by Richman and Marciniec [1990]. As demonstrated in Figures 3 and 4, two steady, fully developed flows are possible in both cases. The light curves correspond to

the less massive of the two flows and the dark curves correspond to the more massive of the two. In the first case (shown in Figures 5, 6, and 7), the mass hold-ups for the two numerical solutions are $m_t$=2.81 and 5.88 and for the two approximate solutions are $m_t$=2.95 and 6.30. In the second case (shown in Figures 8, 9, and 10) the numerical values are $m_t$=3.38 and 8.89, and the approximate values are $m_t$=3.39 and 9.78.

Figures 5 and 8 demonstrate that the approximate solid fraction profiles reach zero at finite distances from the base, whereas the exact profiles vanish only as the distance from the base becomes unbounded. The approximate solutions corresponding to the dilute and dense flows shown in Figures 5, 6, and 7, for example, predict depths 18.58 and 12.65 particle diameters, respectively. Although the corresponding numerical solutions include no such predictions, they do demonstrate that 95.2 percent of the mass of the dilute flow and 99.99 percent of the mass of the dense flow are contained within the depths predicted by the approximate analysis. Similarly, the approximate dilute and dense profiles shown in Figures 8, 9, and 10 have depths of 33.6 and 19.8 particle diameters respectively, while the numerical solutions contain 93.3 and 95.5 percent of the total mass of the corresponding flows within these depths. Consequently, although the exact profiles of w and u extend indefinitely above the base whereas their approximate counterparts end abruptly, this discrepancy is not serious. In

order to emphasize this fact, we have indicated the locations at which $\nu$=.01 by solid dots on the numerically obtained profiles of u and w shown in Figures 6, 7, 9, and 10.

# References

Jenkins, J.T., Richman, M.W., 1985, Grad's 13 Moment System for a Dense Gas of Inelastic Spheres, Arch. Rat. Mech. Anal., Vol. 87, pp. 355-377.

Johnson, P.C., Nott, P., Jackson, R., 1990, Frictional-Collisional Equations of Motion for Particulate Flows and their Applications to Chutes, J. Fluid Mech., Vol. 210, pp. 501-535.

Richman, M.W., 1988, Boundary Conditions Based Upon a Modified Maxwellian Velocity Distribution for Flows of Identical, Smooth, Nearly Elastic Spheres, Acta Mech., Vol. 75, pp. 227-240.

Richman, M.W., Marciniec, R.P., 1990, Gravity-Driven Granular Flows of Smooth, Inelastic Spheres Down Bumpy Inclines, J. Appl. Mech., Vol. 112, pp. 1036-1043.

# Figure Captions

Figure 1: The variations of $\dot{m}$ with W for $\phi$=19.00°, 20.04°, 20.70°, 21.00°, and 21.50° when e=.8, $e_w$=.95, r=1/2, and $\Delta=-1+\sqrt{2}$.

Figure 2: The variations of $\dot{m}$ with W for $\phi$=11.56°, 11.80°, 12.00°, 12.20°, and 12.90° when e=.95, $e_w$=.8, r=1/2, and $\Delta=-1+\sqrt{2}$.

Figure 3: The exact (solid) and approximate (dashed) variations of $\dot{m}$ with $m_t$ for $\phi$=20.70° when e=.8, $e_w$=.95, r=1/2, and $\Delta=-1+\sqrt{2}$. Approximate results were obtained by Richman and Marciniec [1990].

Figure 4: The exact (solid) and approximate (dashed) variations of $\dot{m}$ with $m_t$ for $\phi$=12.20° when e=.95, $e_w$=.8, r=1/2, and $\Delta=-1+\sqrt{2}$. Approximate results were obtained by Richman and Marciniec [1990].

Figure 5: The exact (dark and light solid) and approximate (dark and light dashed) variations of $\nu$ with $Y=y-\beta$ for $\phi$=20.70° and $\dot{m}$=50 when e=.8, $e_w$=.95, r=1/2, and $\Delta=-1+\sqrt{2}$. Approximate results were obtained by Richman and Marciniec [1990].

Figure 6: The exact (dark and light solid) and approximate (dark and light dashed) variations of w with $Y=y-\beta$ for $\phi$=20.70° and $\dot{m}$=50 when e=.8, $e_w$=.95, r=1/2, and $\Delta=-1+\sqrt{2}$. Approximate results were obtained by Richman and Marciniec [1990]. Solid dots indicate where $\nu$=.01.

Figure 7: The exact (dark and light solid) and approximate (dark and light dashed) variations of u with $Y=y-\beta$ for $\phi$=20.70° and $\dot{m}$=50 when e=.8, $e_w$=.95, r=1/2, and $\Delta=-1+\sqrt{2}$. Approximate results were obtained by Richman and Marciniec [1990]. Solid dots indicate where $\nu$=.01.

# Figure Captions (cont.)

Figure 8: The exact (dark and light solid) and approximate (dark and light dashed) variations of $\nu$ with $Y=y-\beta$ for $\phi=12.20°$ and $\dot{m}=50$ when $e=.95$, $e_w=.8$, $r=1/2$, and $\Delta=-1+\sqrt{2}$. Approximate results were obtained by Richman and Marciniec [1990].

Figure 9: The exact (dark and light solid) and approximate (dark and light dashed) variations of w with $Y=y-\beta$ for $\phi=12.20°$ and $\dot{m}=50$ when $e=.95$, $e_w=.8$, $r=1/2$, and $\Delta=-1+\sqrt{2}$. Approximate results were obtained by Richman and Marciniec [1990]. Solid dots indicate where $\nu=.01$.

Figure 10: The exact (dark and light solid) and approximate (dark and light dashed) variations of u with $Y=y-\beta$ for $\phi=12.20°$ and $\dot{m}=50$ when $e=.95$, $e_w=.8$, $r=1/2$, and $\Delta=-1+\sqrt{2}$. Approximate results were obtained by Richman and Marciniec [1990]. Solid dots indicate where $\nu=.01$.

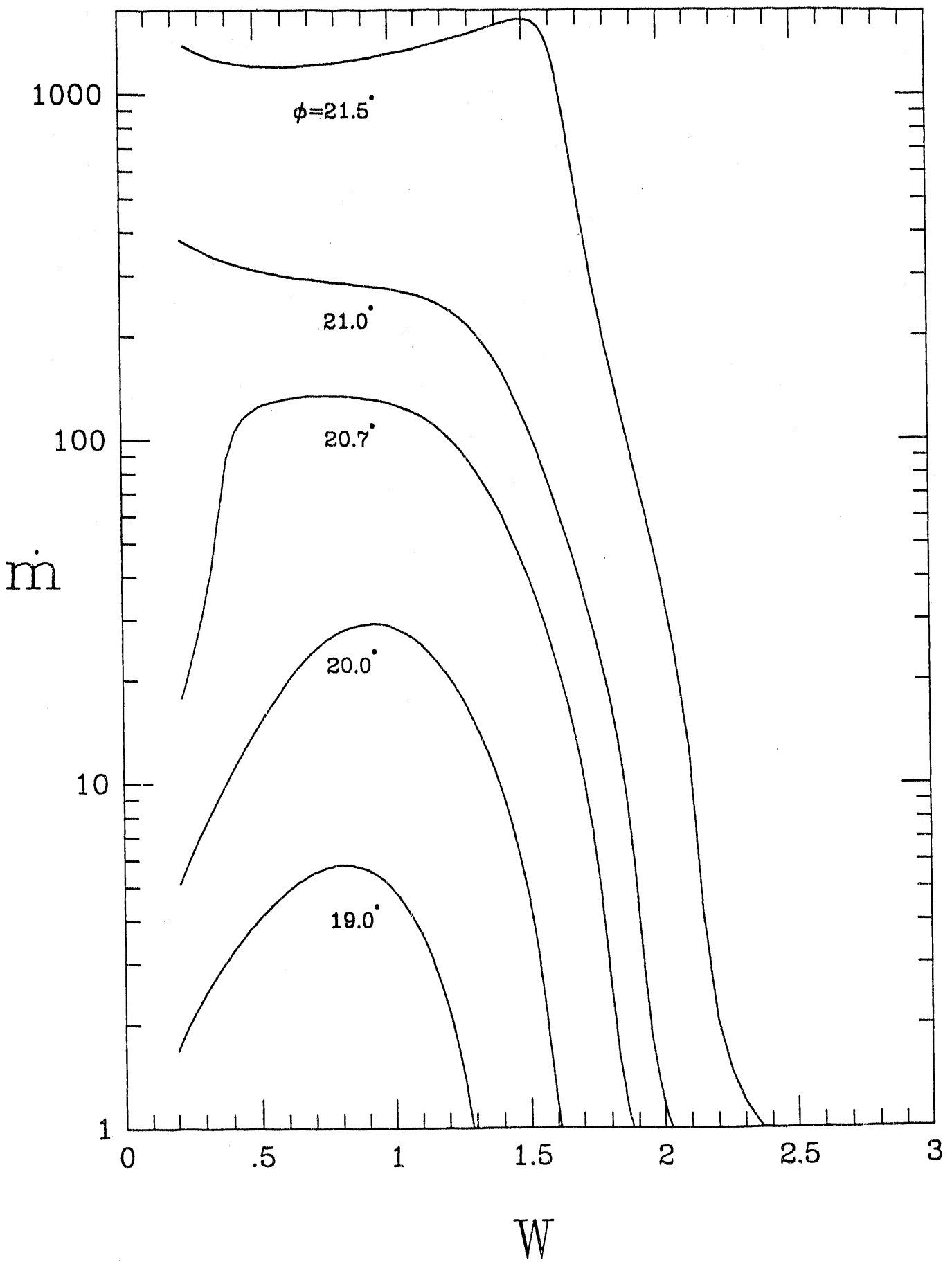


Figure 1.

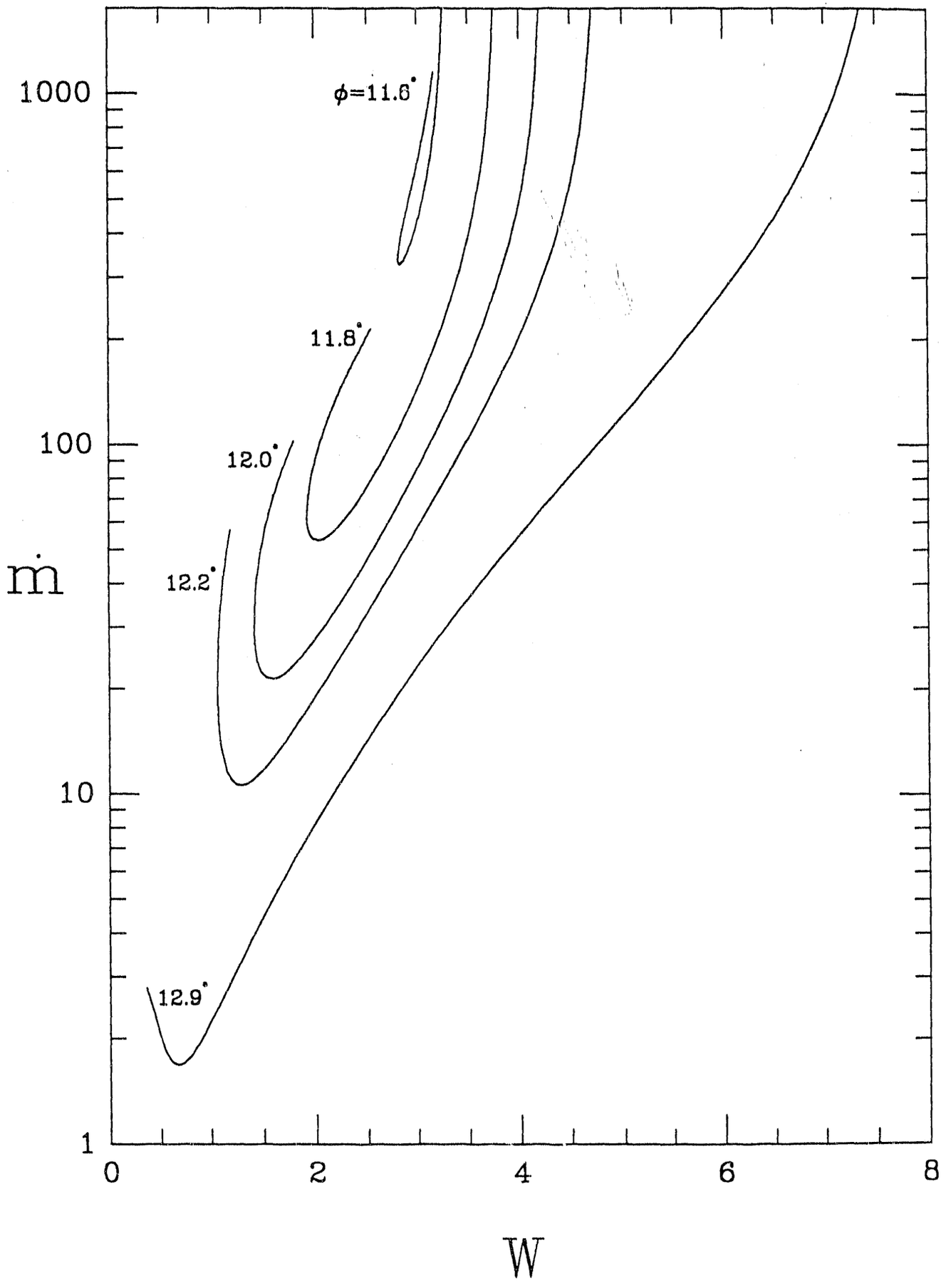


Figure 2.

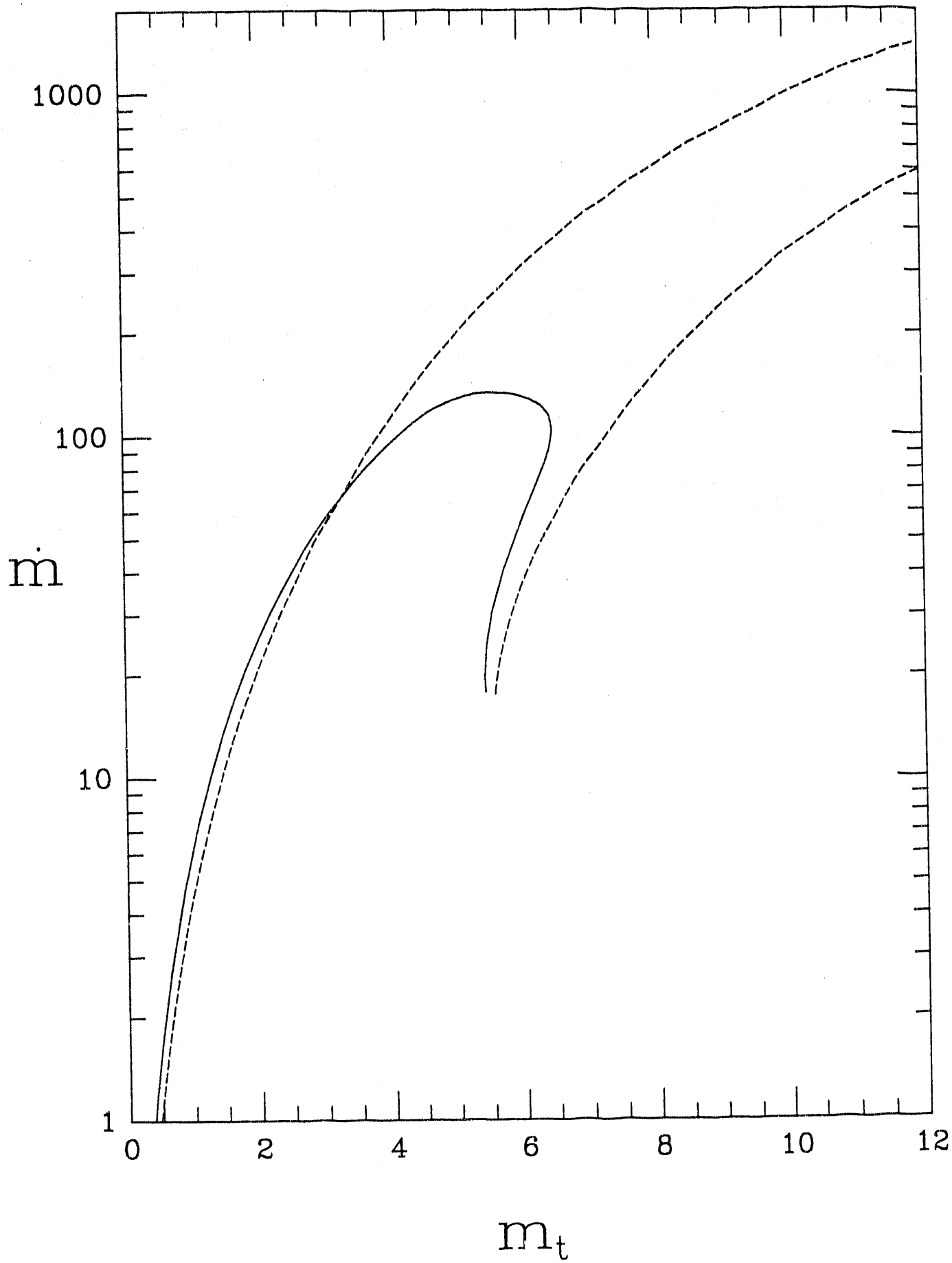


Figure 3.

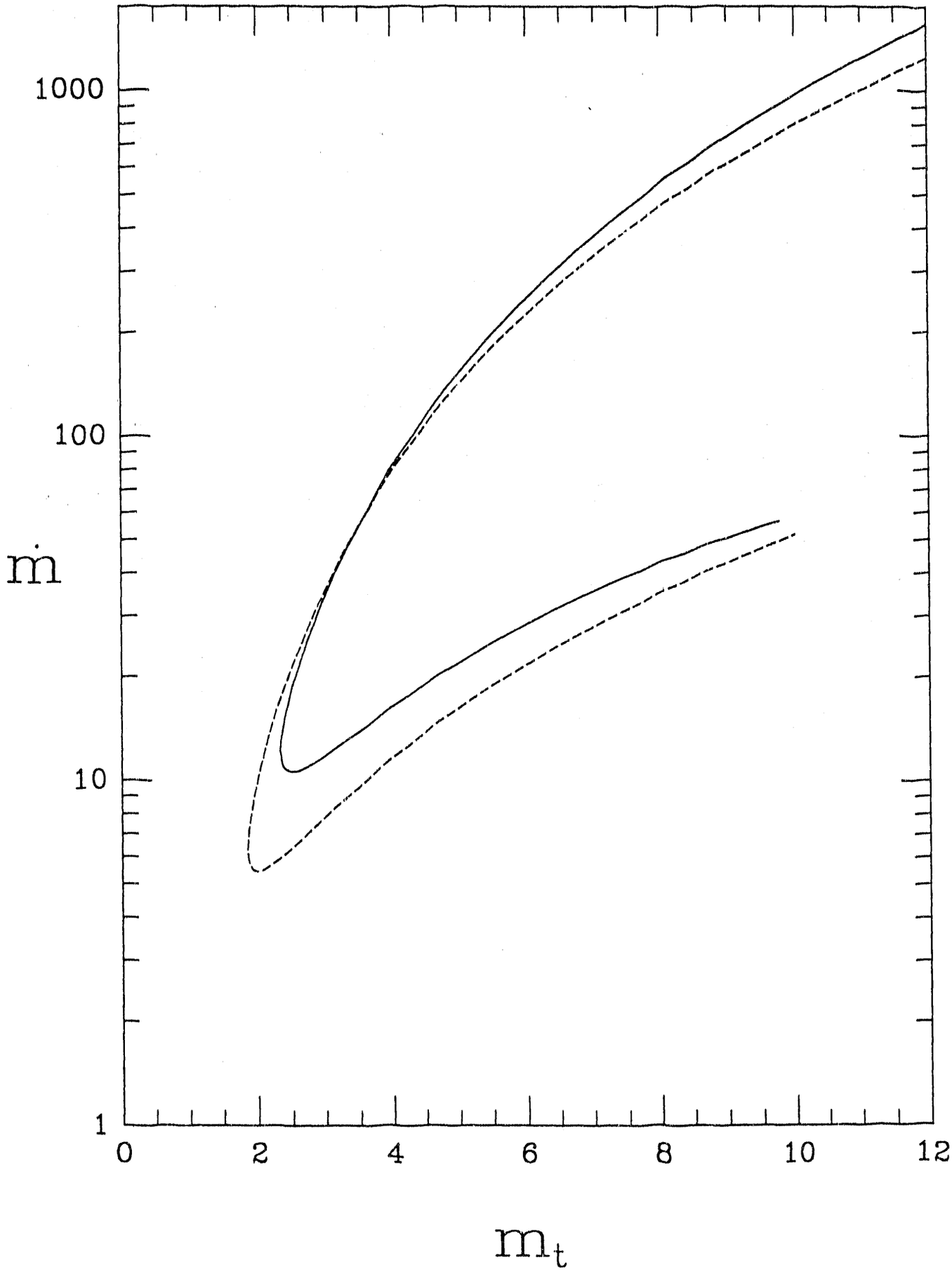


Figure 4.

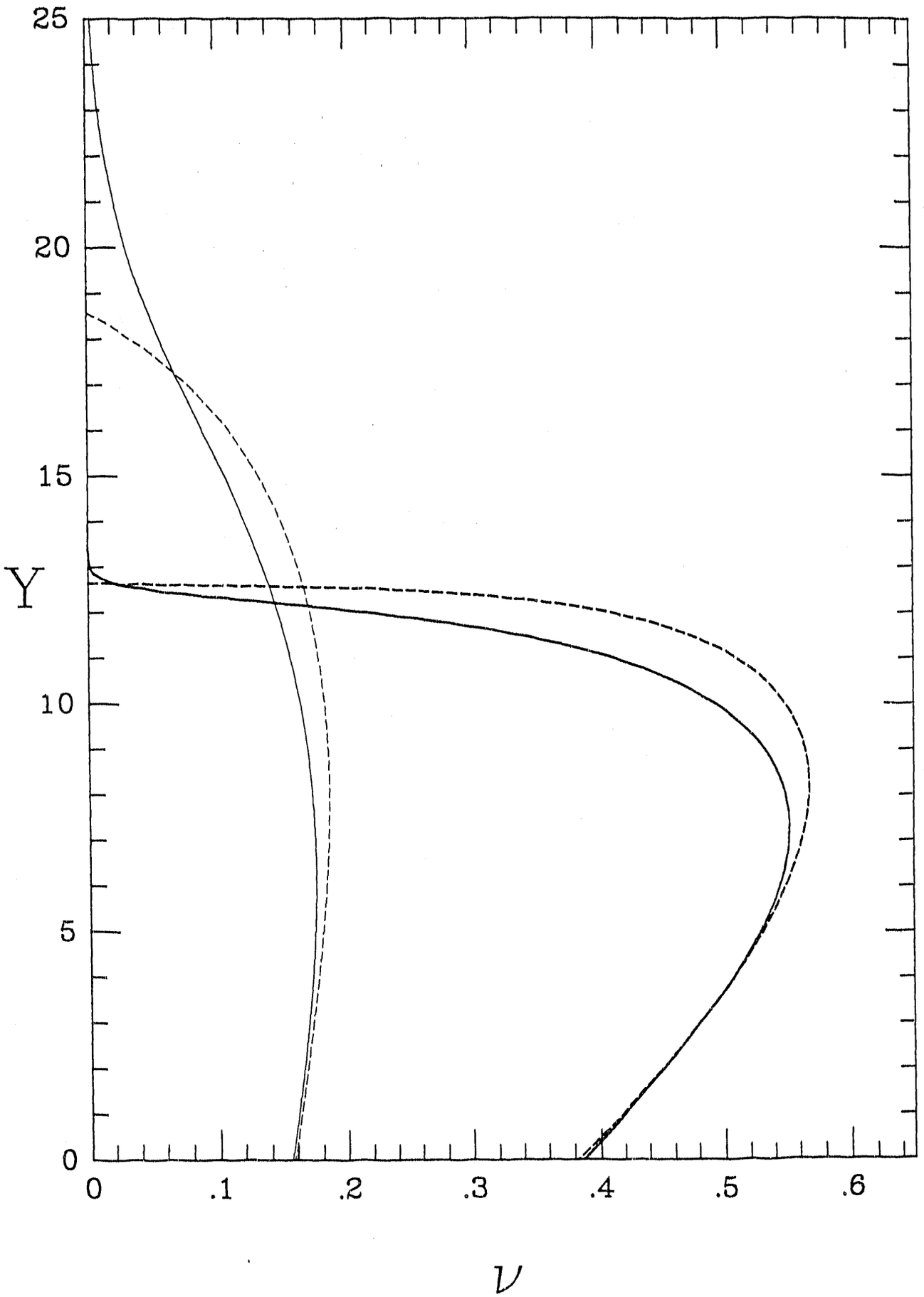


Figure 5.

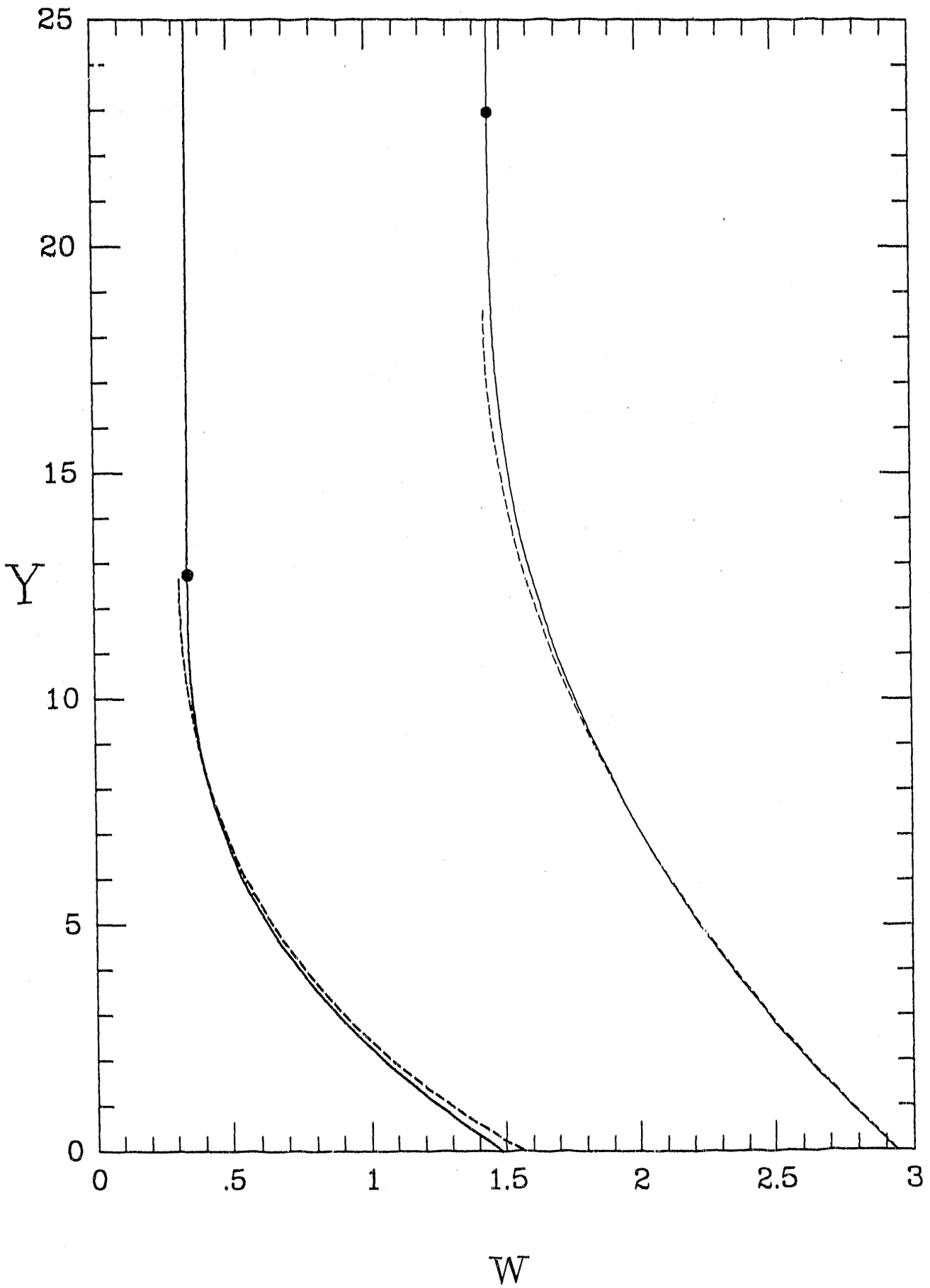


Figure 6.

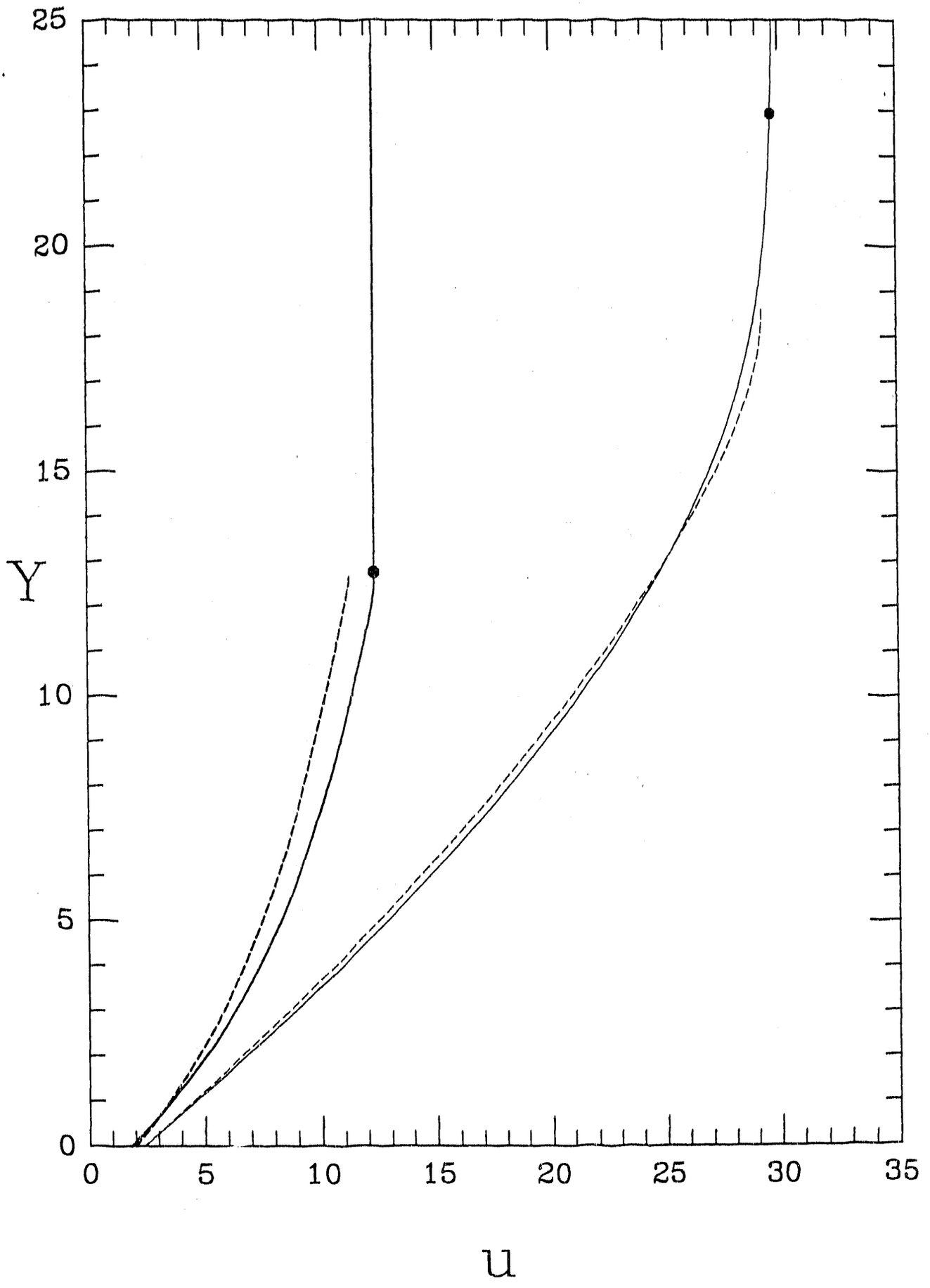


Figure 7.

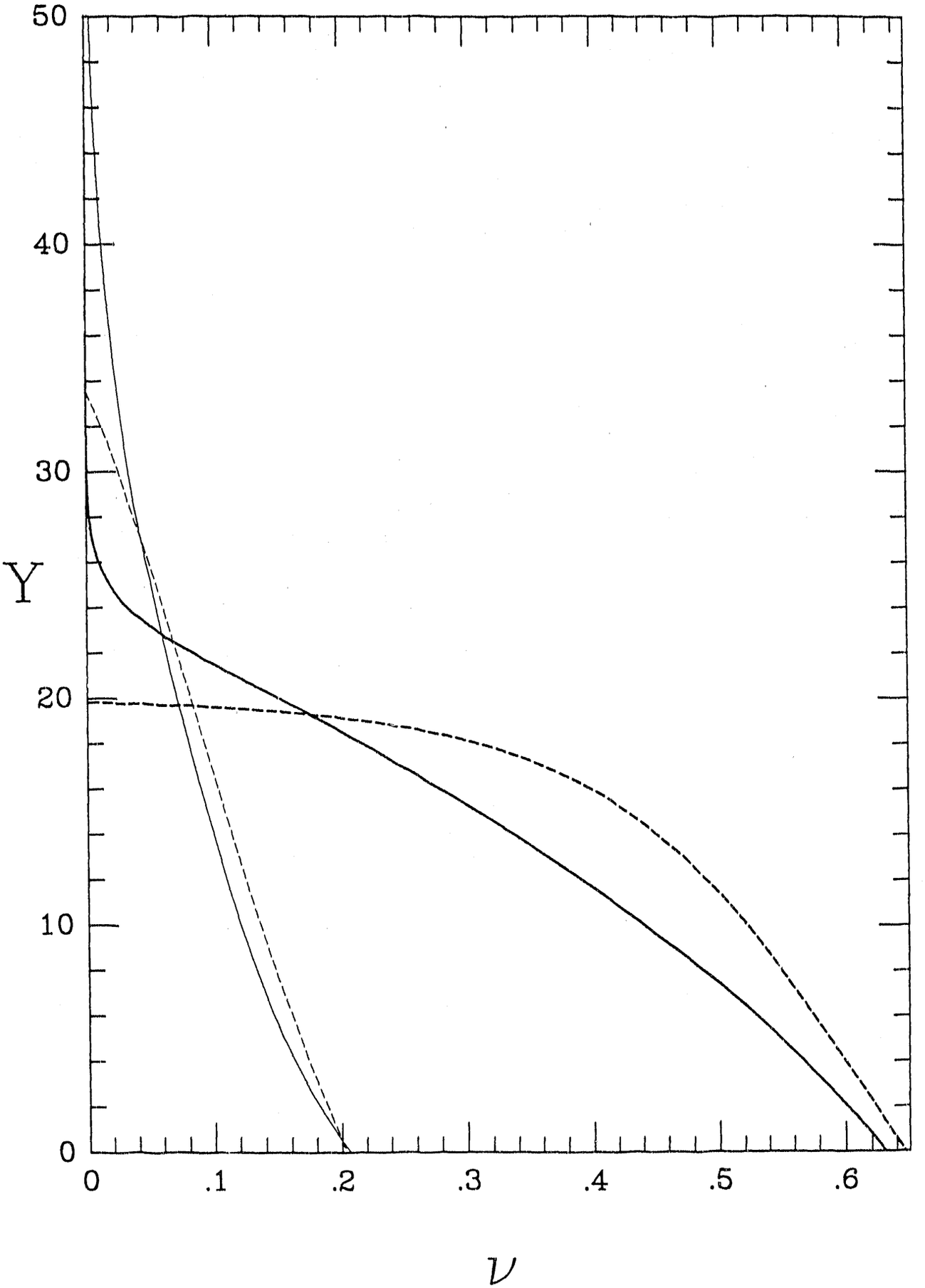


Figure 8.

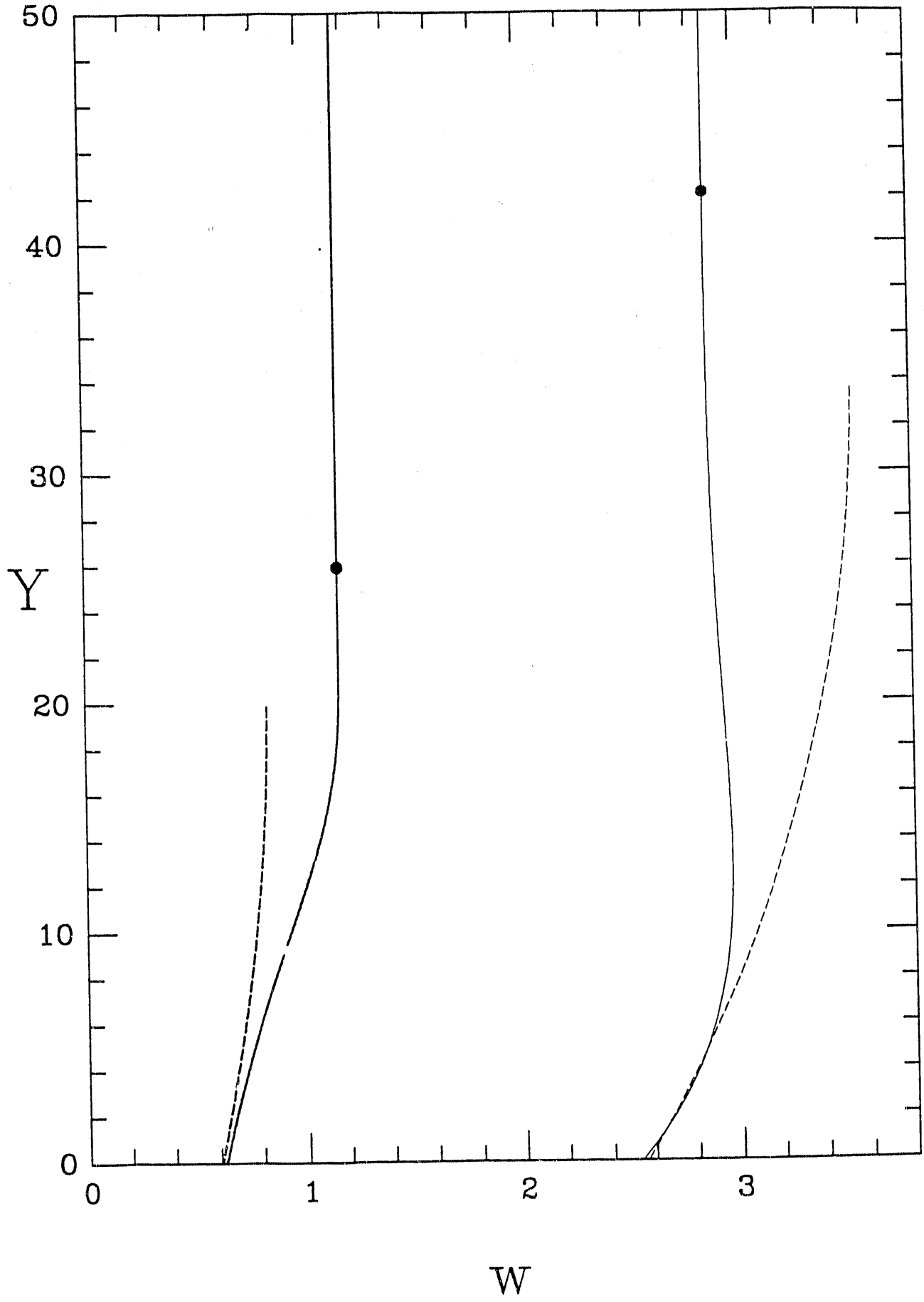


Figure 9.

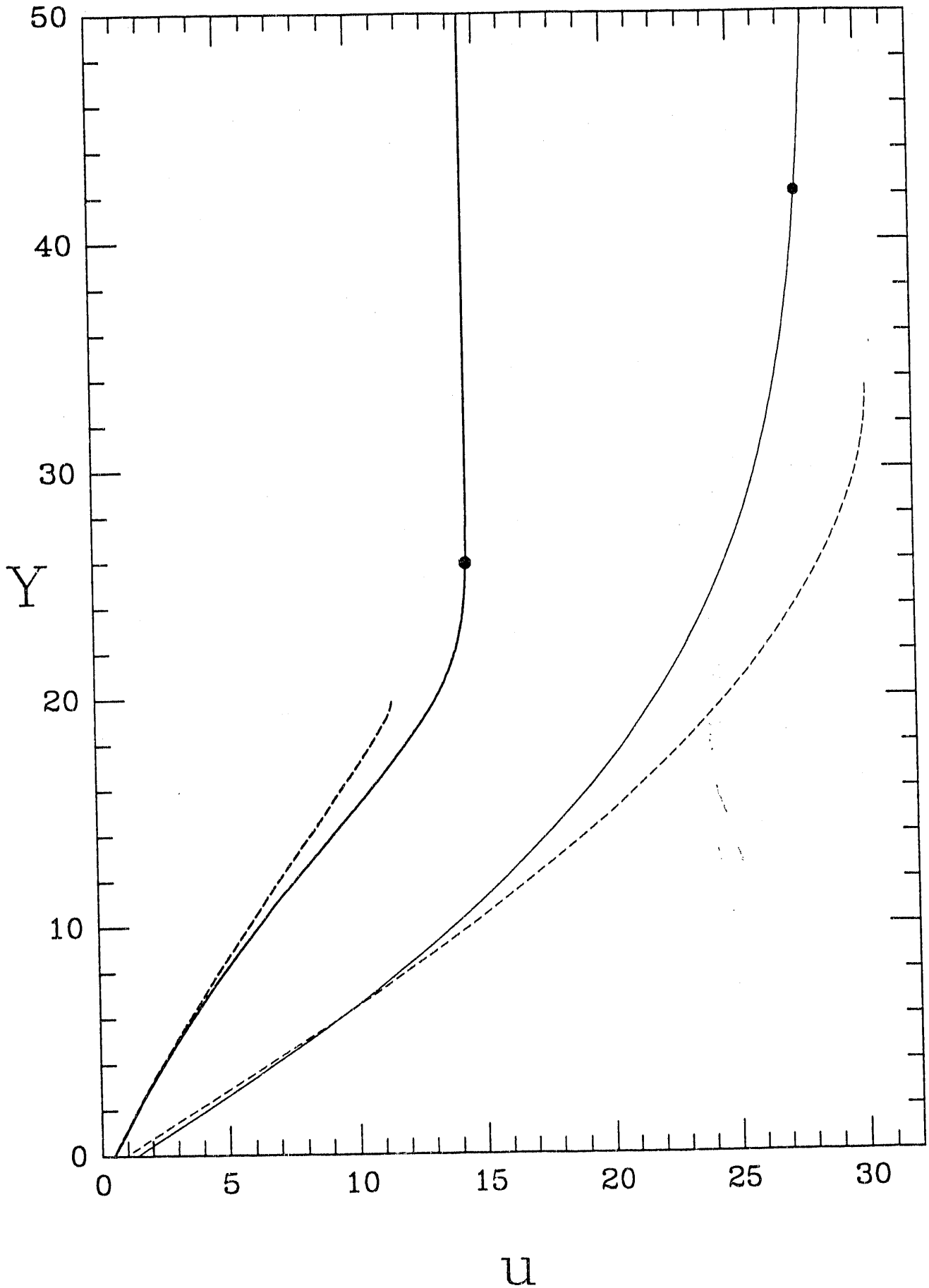


Figure 10.

# END

# DATE FILMED

6/12/92